Materials Science and Engineering C 62 (2016) 558–563

Contents lists available at ScienceDirect

Materials Science and Engineering C

journal homepage: www.elsevier.com/locate/msec

Effect of ultrafine grain on tensile behaviour and corrosion resistance of the duplex stainless steel

Lv Jinlong [a,b,*], Liang Tongxiang [a,b], Wang Chen [a,b], Dong Limin [a,b]

[a] Beijing Key Laboratory of Fine Ceramics, Institute of Nuclear and New Energy Technology, Tsinghua University, Zhongguancun Street, Haidian District, Beijing 100084, China
[b] State Key Lab of New Ceramic and Fine Processing, Tsinghua University, Beijing 100084, China

ARTICLE INFO

Article history:
Received 28 October 2015
Received in revised form 2 January 2016
Accepted 3 February 2016
Available online 5 February 2016

Keywords:
Duplex stainless steel
Grain refinement
Tensile behaviour
Corrosion
Passive film

ABSTRACT

The ultrafine grained 2205 duplex stainless steel was obtained by cold rolling and annealing. The tensile properties were investigated at room temperature. Comparing with coarse grained stainless steel, ultrafine grained sample showed higher strength and plasticity. In addition, grain size changed deformation orientation. The strain induced α′-martensite was observed in coarse grained 2205 duplex stainless steel with large strain. However, the grain refinement inhibited the transformation of α′-martensite;nevertheless, more deformation twins improved the strength and plasticity of ultrafine grained 2205 duplex stainless steel. In addition, the grain refinement improved corrosion resistance of the 2205 duplex stainless steel in sodium chloride solution.

1. Introduction

The duplex stainless steel was currently an alternative to traditional austenitic stainless steel due to its high strength, acceptable plasticity and lower nickel concentration [1]. The lower nickel concentration made it advantageous as a biomaterial in the human body. The mechanical properties of the duplex steels depended strongly on stresses partitioning between austenitic and ferritic grains as well as morphological and crystallographic textures in ferrite and austenitic phases [2]. These superior performances originated from a mixture of austenitic and ferritic phases. Jiménez et al. [3] suggested that superplastic properties of austenite/ferrite stainless steel were attributed to grain boundary sliding. In situ tensile tests from atomic force microscope showed that plane slips occurred at austenitic grains in a low strain level for austenitic–ferritic duplex stainless steel. The slip lines with different orientations were distributed homogeneously within all the austenitic grains, while only a few signs of plastic deformation were activated in ferritic grains in a high strain level [4]. The number of slip bands in both phases increased with the applied plastic strain for duplex stainless steel [5]. In situ observations revealed that the plastic deformation occurred within the soft austenitic phase at the beginning of the deformation stage, while plastic deformation occurred by slip gliding in the ferritic phase with the increasing of the strain [6]. Grains with almost identical crystallographic orientation of the ferrite grains experienced large differences in lattice strain [7]. The deformation twinning and martensite were formed in austenitic phase in an UNS S32304 duplex stainless steel subjected to equal channel angular pressing [8]. Nanocrystalline duplex stainless steel with a grain size of about 150 nm in ferrite and 70 nm in austenite was obtained by hydrostatic extrusion [9]. The ultimate strength appeared to increase significantly. However, the plasticity significantly decreased.

The mechanical behaviour of the stainless steel orthodontic wire and its corrosion resistance in simulated saliva solution were both very important problems [10]. Up to date, there is no study to investigate the effect of grain refinement of 2205 duplex stainless steel on its corrosion resistance. Therefore, the objective of this work was to evaluate the effect of ultrafine grain on tensile property of the 2205 duplex stainless steel and its corrosion resistance in the chlorine ion environment.

2. Experimental procedure

2.1. Sample preparation and characterization

The chemical composition of 2205 duplex stainless steel in weight percent was 0.05 C, 1.05 Mn, 0.022 P, 0.0008 S, 0.75 Si, 21.85 Cr, 5.36 Ni, 3.18 Mo, 0.18 Cu, 0.13 V, 0.054 W, 0.015 Ti, 0.155 N and Fe balance. The as-received samples were annealed at 1100 °C for 1 h and water-quenched. The ultrafine grained 2205 duplex stainless steel was obtained by 95 ± 0.5% total thickness reduction in a laboratory rolling mill and annealed at 900 °C to up to 300 s. Tensile tests were conducted at

* Corresponding author at: Beijing Key Laboratory of Fine Ceramics, Institute of Nuclear and New Energy Technology, Tsinghua University, Zhongguancun Street, Haidian District, Beijing 100084, China.
E-mail addresses: ljltsinghua@126.com (L. Jinlong), txliang@mail.tsinghua.edu.cn (L. Tongxiang).

http://dx.doi.org/10.1016/j.msec.2016.02.008
0928-4931/

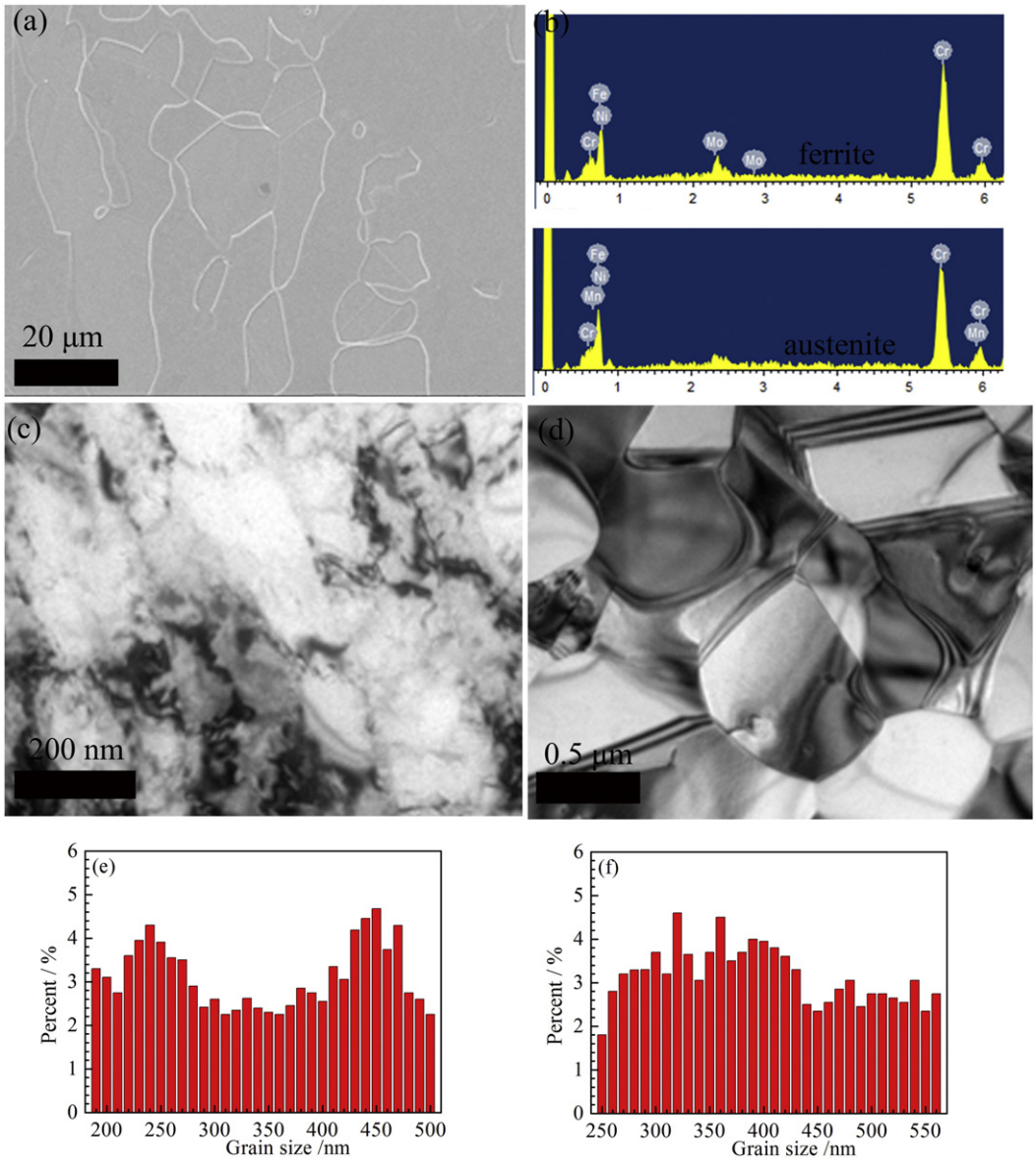

Fig. 1. The microstructure of (a) solid solution 2205 duplex stainless steel, (b) chemical composition of austenitic and ferritic phases, and (c) cold rolled and (d) annealed 2205 duplex stainless steels. The statistical distributions for grain size of (e) ferritic and (f) austenitic phases, respectively.

ambient temperature at a strain rate of $1 \times 10^{-4}\ s^{-1}$. The tensile direction was parallel to the rolling direction of the samples. The phase transformation was analysed by X-ray diffraction (XRD) with CuK_{α} radiation. A JEM-2100F transmission electron microscopy (TEM) was used to examine the microstructure of the grain. The samples for TEM observation were prepared using a twin-jet electropolishing at a voltage of 20 V at a temperature of −25 °C. The electrolyte contained 10 vol.% of perchloric acid and 90 vol.% of alcohol. The microhardness of the austenitic and ferritic phases in coarse grained 2205 duplex stainless steels from the center of the grain was tested by a Vickers hardness tester with a load of 100 g for 10 s dwell time. While microhardness of the ultrafine grained sample was measured randomly. At least three points of each phase in every test area were measured and the average value was obtained.

2.2. Electrochemical tests

The samples were successively ground with SiC paper up to a grit of #2000, polished with alumina slurry down to 0.3 μm. The polished samples were ultrasonically cleaned in acetone and ethanol. Electrochemical tests were performed with a CHI 660E electrochemical station

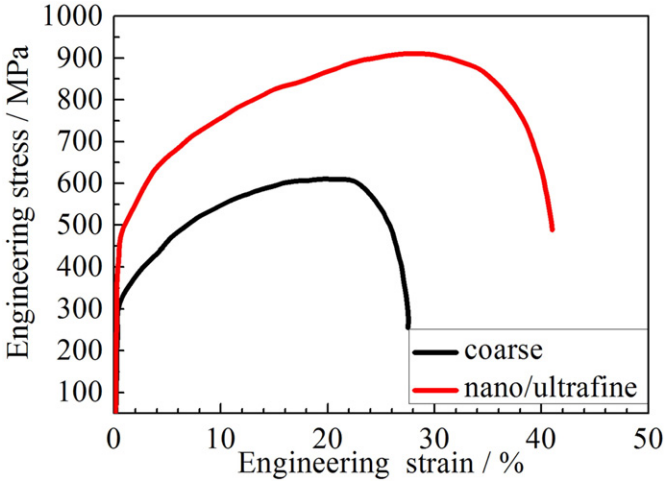

Fig. 2. Comparison of engineering stress–strain plots for coarse grained and ultrafine grained 2205 duplex stainless steels.

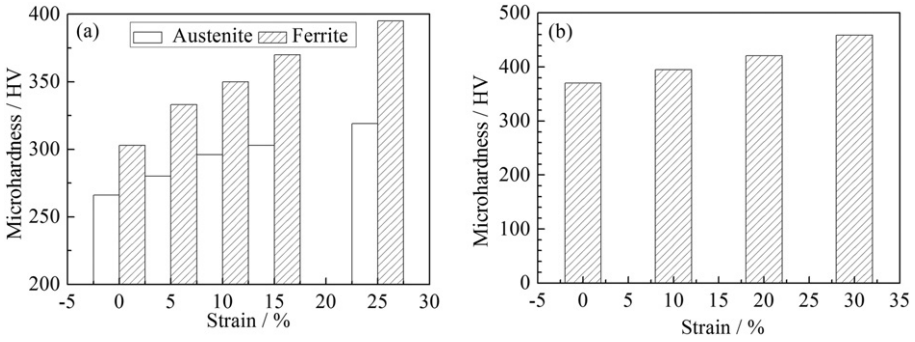

Fig. 3. Effect of tensile on the Vickers microhardness of (a) coarse grained and (b) ultrafine grained 2205 duplex stainless steels, respectively.

(Chenhua instrument Co. Shanghai, China) controlled by a computer and software in a three-electrode cell. The electrochemical measurements were conducted using a three-electrode cell comprising a thin platinum plate as the counter electrode, a saturated calomel electrode (SCE) as the reference electrode and the stainless steel as the working electrode. All the potentials referred in this work were measured with respect to the value of SCE. The electrochemical experiments were carried out in 0.1 M NaCl solution. Before the experiment samples were cathodically polarized at −1.2 V_{SCE} for 300 s to remove the natural passive film. The potential swept rate of the potentiodynamic polarization curves in anodic direction was 1 mV s^{-1}. The electrochemical impedance spectroscopy (EIS) measurements were carried out using a frequency range of 100 kHz to 10 mHz and with a 5 mV amplitude of the AC signal.

3. Results and discussion

The coarse grained 2205 duplex stainless steel is shown in Fig. 1a. The microstructure of the solution annealed sample shows a bulgy ferrite phase and concave austenite phase. The result of Energy Dispersive Spectrometer shows that the chromium and molybdenum enrich ferritic phase, while nitrogen and nickel enrich austenitic phase in Fig. 1b. After the cold rolling, a lot of austenite grains are transformed into α′-martensite in Fig. 1c. α′-Martensite contains high density dislocations. The XRD result also shows diffraction peak of α′-martensite (not shown here). In addition, ferrite grains are also significantly refined. The dislocation slip is the main mechanism of grain refinement by the dislocation cell and dislocation substructure. In the early stage of deformation, austenitic phase underwent rapid grain subdivision caused by twinning and the generation of dislocations [11]. During the large deformation stage, the dislocation structures could transform into grains. The refinement of the microstructure in the austenitic phase was much more obvious than that in ferritic one. After annealing, ultrafine 2205 duplex stainless steels with the average size of 480 nm are obtained in Fig. 1d. The strain induced α′-martensite could be formed during low-cycle fatigue [12] and cold rolling for duplex stainless steels [13]. A large number of α′-martensites were produced due to the preferential deformation of austenite. However, the compression results also confirmed that the strength of ferritic phase was higher than the austenitic phase [14]. Considering the very high hardness of strain induced α′-martensite, high dislocation density in ferritic phase could induce its high hardness. Mechanical properties of 2205 duplex stainless steel were directly affected by the initial microstructures [15]. Moreover, grain size and grain orientation change will undoubtedly affect its hardness. The change of microstructures will be investigated by the following TEM observation. The statistical distributions of ferritic phase and austenitic phase are shown in Fig. 1e and f, respectively. Comparing with austenitic phase, double grain distribution is observed in ferritic phase. Moreover, the austenitic phase is slightly coarser than ferritic phase. It can be found that the austenitic grain is more uniform than ferritic grain.

True stress–strain plots of the coarse grained and ultrafine grained 2205 duplex stainless steels are showed in Fig. 2. It can be seen that the yield strength and elongation of ultrafine grained 2205 stainless steel are much higher than those of coarse grained one. The yield strength and elongation is 452 MPa and 39% for ultrafine grained 2205 duplex stainless steel, while the corresponding value is 310 MPa and 26% for coarse grained one. Misra et al. [16] studied and found that nano/ultrafine 304 stainless steel showed higher strength than coarse grained one. They suggested that improved strength was attributed to increased stability of austenitic phase due to a decrease in grain size. Our study indicates that grain refinement improves both strength and plasticity of the 2205 stainless steel.

Fig. 3a shows the microhardness values of austenitic and ferritic phases in coarse grained 2205 duplex stainless steels. Note that increasing of the microhardness value in ferritic phases is more significant than that in austenitic phase. This indicates that the tensile strain has a greater effect on ferritic phase than austenitic phase. The ultrafine grained 2205 duplex stainless steel has higher microhardness than coarse grained one with the increasing of strain in Fig. 3b. The increasing in hardness is attributed to the grain refinement and the change of microstructures. Comparing with coarse grained 2205 duplex stainless steel,

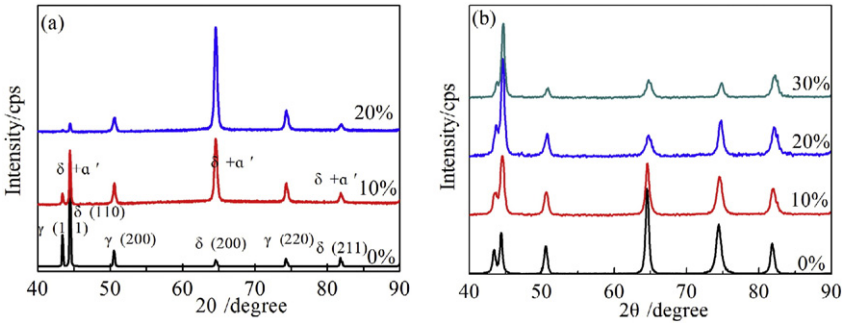

Fig. 4. X-ray diffraction patterns for (a) coarse grained and (b) ultrafine grained 2205 duplex stainless steels with different strains.

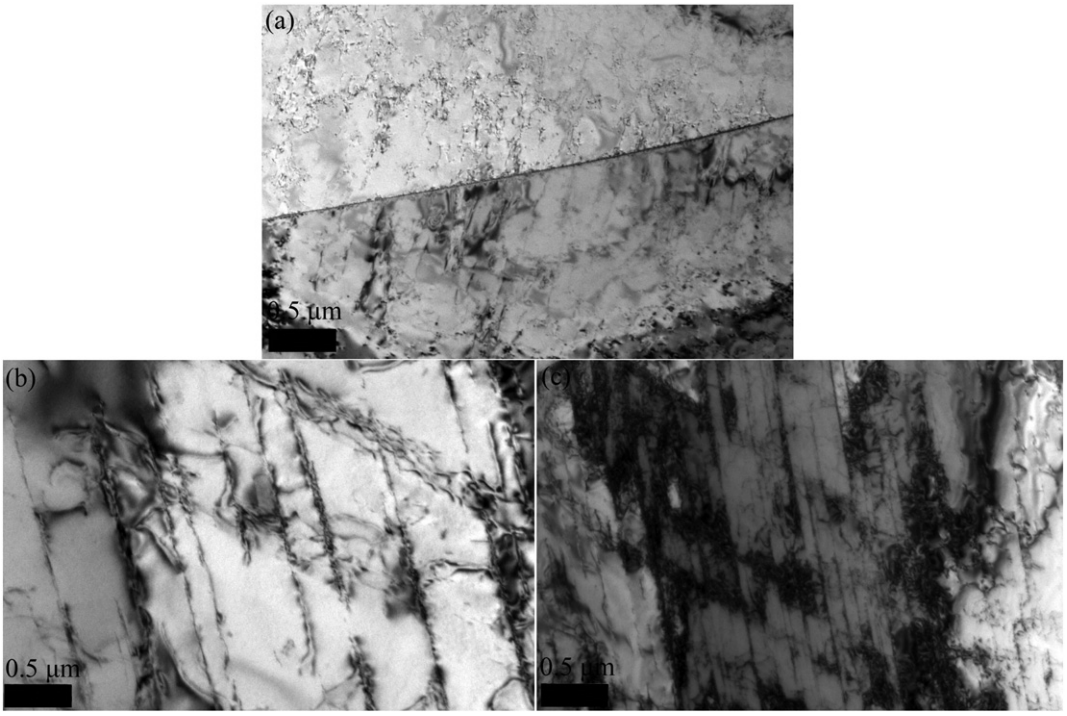

Fig. 5. Representative TEM micrographs of coarse grained 2205 duplex stainless steel with (a) 5%, (b) 10%, and (c) 20% strain, respectively.

mechanical behaviour of ultrafine grained one is improved significantly. Therefore, XRD and TEM techniques are used to examine the deformed structures.

The diffraction peak intensities of α′-martensite and ferritic phase increase with the increasing of strain in Fig. 4a and b. Comparing Fig. 4a with Fig. 4b, it can be found that preferred orientation of ferritic phase in coarse grained 2205 duplex stainless steel is (110), while preferred orientation of ferritic phase in ultrafine grained 2205 duplex stainless steel is (200). The preferred orientation of ferritic phase in deformed coarse grained and ultrafine grained 2205 duplex stainless steels is (200) and (110), respectively. The investigation shows that the grain refinement by the thermomechanical process changes the grain orientation, moreover, the deformation process also affects the grain orientation of the two samples.

Some dislocations occur inside the grain in coarse grained 2205 duplex stainless steel with small strain in Fig. 5a. With the increasing of

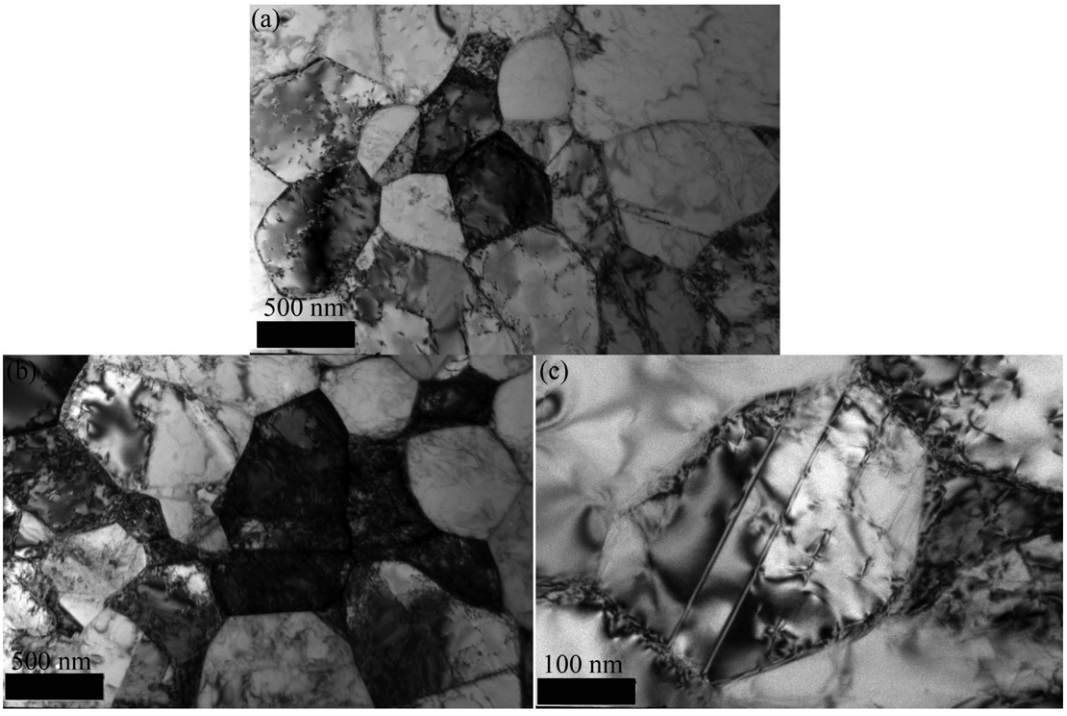

Fig. 6. Representative TEM micrographs of ultrafine grained 2205 duplex stainless steel with (a) 10%, (b) 20%, and (c) 30% strain, respectively.

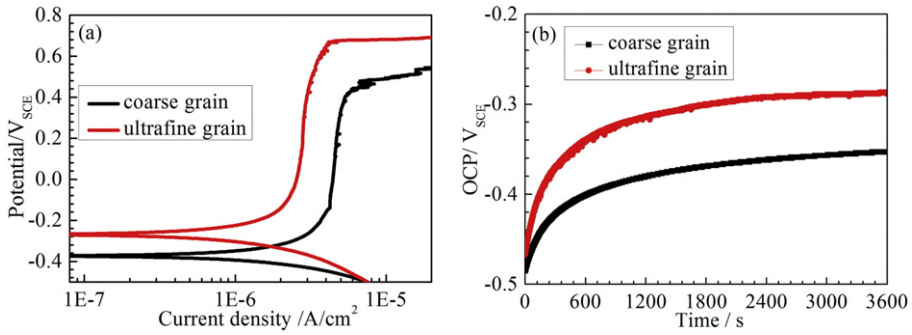

Fig. 7. (a) The potentiodynamic polarization curves and (b) the OCP for coarse grained and ultrafine grained 2205 duplex stainless steels in 0.1 M NaCl solution.

strain, the dislocation density increases in two phases, Moreover, tangle of dislocation occurs in the austenitic grains in Fig. 5b. Many shear bands occur in the austenite grains with the further increasing of strain in Fig. 5c. In addition, some intersections of shear bands act as the nucleation sites for α′-martensite. The analytical transmission electron microscopy studies showed that martensitic transformation mechanisms of the austenitic phase included γ (fcc) → ε (hcp), γ(fcc) → α′ (bcc) and γ (fcc) → ε (hcp) → α′ (bcc) [17]. Cao et al. found that the neighbouring ferrite and austenite always maintained similar hardness during plastic deformation [18]. Moreover, the plastic deformation of ferritic phase occurred mainly via dislocation activities, while the plastic deformation of austenitic phase evolved by dislocation slip and deformation twinning. Grain refinement could affect the deformation mechanism and further affect the mechanical properties.

Fig. 6a–c show microstructures of ultrafine grained 2205 duplex stainless steels with different strain levels. Some planar dislocations occur at intragranular and grain boundaries in Fig. 6a. The dislocation density increases due to higher strain in Fig. 6b. Deformation twinning is activated in ultrafine grained 2205 duplex stainless steels due to large strain in Fig. 6c.

The interactions between the dislocations and twin boundaries play a significant role in the plastic deformation process for ultrafine grained 2205 duplex stainless steel, especially for sample with large strain. Once the dislocations are emitted at the boundaries, then they move through the grain interior. This process can improve plasticity [19]. When dislocations are blocked at twin boundaries, higher stress is needed to make dislocations pass through twin boundaries, which results in higher tensile strength. Moreover, more deformation twins in ultrafine grained 2205 duplex stainless steel inhibit dislocation slip and α′-martensite transformation. Grain refinement inhibits the transformation of α′-martensite for 2205 duplex stainless steel. This was attributed to a fact that the α′-martensite transformation was saturated because of the austenitic grain refinement and the increasing of austenite stabilization for a near-Ni-free, Mn–N bearing duplex stainless steel [20]. Comparing with tensile strength (over 1000 MPa) and 50% elongation in Mn–N bearing duplex stainless steel [20], our ultrafine grained 2205 duplex stainless steel showed lower elongation and slightly lower tensile strength. This was mainly attributed to a fact that very low stacking fault energy of austenitic phase in Mn–N bearing duplex stainless steel promoted strain induced α′-martensite transformation. The transformation induced plasticity improved elongation of Mn–N bearing duplex stainless steel [20]. However, we found that grain refinement of 2205 duplex stainless steel inhibited the transformation of α′-martensite, which resulted in lower elongation. In addition, grain refinement also decreased elongation of 2205 duplex stainless steel. However, the grain refinement of 2205 duplex stainless steel induced deformation twin which improved tensile strength and elongation.

Fig. 7a shows the potentiodynamic polarization curves for coarse grain and ultrafine grained 2205 duplex stainless steel in 0.1 M NaCl solution at room temperature. Both of them have similar anodic polarization behaviour. The corrosion potential of ultrafine grained and coarse grained duplex stainless steels in 0.1 M NaCl solution is −0.268 V_{SCE}, and −0.377 V_{SCE}, respectively, a little positive of the former than the latter is observed. Besides, passive current of ultrafine grained duplex stainless steel is lower than that of the coarse grain one. This implies that the grain refinement affects the structure and composition of the passive films on the surface of duplex stainless steel. Zheng et al. [21] found that thickness and composition of the passive film formed on both as-received and nanocrystalline 304 stainless steel by equal channel angular pressed in 0.5 M H_2SO_4 at room temperature showed little difference. However, more grain boundaries due to grain refinement could improve the chromium diffusion and promoted to the forming of compact passive film. Therefore, Balusamy et al. [22] illustrated that nanocrystallisation induced by a surface mechanical attrition treatment increased the corrosion resistance of 409 stainless steels.

The corrosion resistance of coarse grained and ultrafine grained 2205 duplex stainless steels in 0.1 M NaCl solution is also evaluated by open circuit potential (OCP) tests. Fig. 7b shows that the OCP shifts to more positive potential in two samples. The OCP of ultrafine grained 2205 duplex stainless steel was higher than that of coarse grained one in 0.1 M NaCl solution. The more positive value of the OCP could be attributed to thickening of the passive film spontaneously formed on the

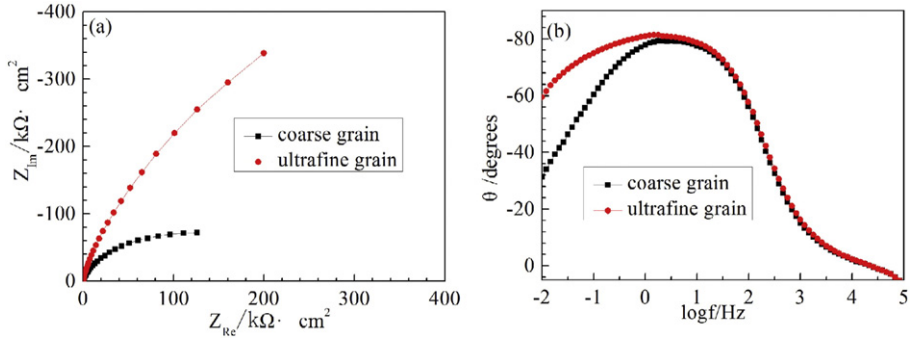

Fig. 8. (a) Nyquist and (b) Bode plots for coarse grained and ultrafine grained 2205 duplex stainless steels in 0.1 M NaCl solution.

surface or more compactness and stability of the passive film [23]. This conjecture is subsequently confirmed by the following experiments.

Typical Nyquist plots of coarse grained and ultrafine grained 2205 duplex stainless steels in 0.1 M NaCl solution are showed in Fig. 8a. The diameter of the semicircle of Nyquist plot is directly proportional to corrosion resistance [24]. This suggests that charge transfer resistance of the passive film increases due to grain refinement for 2205 duplex stainless steels in sodium chloride solution. The Bode plots of two duplex stainless steels are in Fig. 8b. A time constant is observed. The high angles at low frequencies are typical characteristic for passivated materials in Bode plots [25]. The passive film formed on the surface of the 2205 duplex stainless steel has a bilayer structure, predominantly contained Fe species and Cr-oxide [26]. The heterogeneous passive film was formed on both phases of the duplex stainless steel due to the differences in chemical composition between austenitic and ferritic phases [27] .Compared to γ-phase, Fe species in passive film of α-phase were more stable due to the higher content of Mo in α-phase for 2205 duplex stainless steel in neutral 3.5% NaCl solution [28]. However, the superior stability of Cr (III) species in the passive layer of γ-phase might result from the higher content of Ni in γ-phase. In addition, effect of coupling of two phases was beneficial to the passive behaviour of 2205 duplex stainless steel. Therefore, the doping densities, the thickness and chemical compositions of the passive film could affect the corrosion resistance of the 2205 duplex stainless steel in the chlorine ion environment. In the middle frequency region, broadening plateau reveals protective passive films of ultrafine grained 2205 duplex stainless steels in Fig. 8b [29]. These data of EIS test in Fig. 8a and b further support the results from potentiodynamic polarization curves in Fig. 7a and OCP curves in Fig. 7b.

4. Conclusion

The present study investigated the effect of grain refinement of the 2205 duplex stainless steel on its tensile property and corrosion resistance in the chlorine ion environment. The main conclusions were as follows:

1) The ultrafine grained 2205 duplex stainless steel had higher strength and plasticity than coarse grained one.
2) The grain refinement of the 2205 duplex stainless steel inhibited the strain induced α′-martensite transformation and promoted to form more nanotwins.
3) Grain refinement improved corrosion resistance of ultrafine 2205 duplex stainless steel in sodium chloride solution.
4) The grain refinement facilitated the forming of more protective passive films for 2205 duplex stainless steel in the chlorine ion environment.

Acknowledgements

This work was financially supported by the National Natural Science Foundation of China (Grant No. 91326203).

References

[1] N. Ebrahimi, M. Momeni, M.H. Moayed, A. Davoodi, Corros. Sci. 3 (2011) 637–644.
[2] J.J. Moverare, M. Odén, Mater. Sci. Eng. A 337 (2002) 25–38.
[3] J.A. Jiménez, G. Frommeyer, M. Carsí, O.A. Ruano, Mater. Sci. Eng. A 307 (2001) 134–142.
[4] S. Fréchard, F. Martin, C. Clément, J. Cousty, Mater. Sci. Eng. A 418 (2006) 312–319.
[5] I. Serre, D. Salazar, J.B. Vogt, Mater. Sci. Eng. A 492 (2008) 428–433.
[6] E.Y. Guo, M.Y. Wang, T. Jing, N. Chawla, Mater. Sci. Eng. A 580 (2013) 159–168.
[7] P. Hedström, T.S. Han, U. Lienert, J. Almer, M. Odén, Acta Mater. 58 (2010) 734–744.
[8] L. Chen, F.P. Yuan, P. Jiang, X.L. Wu, Mater. Sci. Eng. A 551 (2012) 154–159.
[9] P. Maj, B. Adamczyk-Cieślak, J. Mizera, W. Pachla, K.J. Kurzydłowski, Mater. Charact. 93 (2014) 110–118.
[10] M. Mirjalili, M. Momeni, N. Ebrahimi, M.H. Moayed, Mater. Sci. Eng. A C 33 (2013) 2084–2093.
[11] T. Morikawa, K. Higashida, T. Sato, ISIJ Int. 42 (2002) 1527–1533.
[12] P.K. Chiu, K.L. Weng, S.H. Wang, J.R. Yang, Y.S. Huang, J. Fang, Mater. Sci. Eng. A 398 (2005) 349–359.
[13] S.S.M. Tavares, M.R. da Silva, J.M. Pardal, H.F.G. Abreu, A.M. Gomes, J. Mater. Process. Technol. 180 (2006) 318–322.
[14] E.Y. Guo, H.X. Xie, S.S. Singh, A. Kirubanandham, T. Jing, N. Chawla, Mater. Sci. Eng. A 598 (2014) 98–105.
[15] S.X. Li, X.P. Ren, X. Ji, Y.Y. Gui, Mater. Des. 55 (2014) 146–151.
[16] R.D.K. Misra, V.S.A. Challa, P.K.C. Venkatsurya, Y.F. Shen, M.C. Somanid, L.P. Karjalainen, Acta Mater. 84 (2015) 339–348.
[17] A. Das, S. Sivaprasad, P.C. Chakraborti, S. Tarafder, Mater. Sci. Eng. A 528 (2011) 7909–7914.
[18] Y. Cao, Y.B. Wang, X.H. An, X.Z. Liao, M. Kawasaki, S.P. Ringer, T.G. Langdon, Y.T. Zhu, Acta Mater. 63 (2014) 16–29.
[19] L. Lu, Y.F. Shen, X.H. Chen, L.H. Qian, K. Lu, Science 304 (2004) 422–426.
[20] J.Y. Choi, J.H. Ji, S.W. Hwang, K.T. Park, Mater. Sci. Eng. A 535 (2012) 32–39.
[21] Z.J. Zheng, Y. Gao, Y. Gui, M. Zhu, Corros. Sci. 54 (2012) 60.
[22] T. Balusamy, S. Kumar, T.S.N. Sankara Narayanan, Corros. Sci. 52 (2010) 3826.
[23] T.M. Yue, L.J. Yan, C.P. Chan, C.F. Dong, H.C. Man, G.K.H. Pang, Surf. Coat. Technol. 179 (2004) 158–164.
[24] H. Ma, S. Chen, L. Niu, S. Zhao, S. Li, D. Li, J. Appl. Electrochem. 32 (2002) 65–72.
[25] M. Chembath, J.N. Balaraju, M. Sujata, Mater. Sci. Eng. C 56 (2015) 417–425.
[26] H. Luo, C.F. Dong, X.G. Li, K. Xiao, Electrochim. Acta 64 (2012) 211–220.
[27] V. Vignal, H. Zhang, O. Delrue, O. Heintz, I. Popa, J. Peultier, Corros. Sci. 53 (2011) 894–903.
[28] Y. Wang, X.Q. Cheng, X.G. Li, Electrochem. Commun. 57 (2015) 56–60.
[29] K.R. Trethewey, M. Paton, Mater. Lett. 58 (2004) 3381–3384.